Comparison of Substrate Specificities of *Escherichia coli* Endonuclease III and Its Mouse Homologue (mNTH1) Using Defined Oligonucleotide Substrates†

Kenjiro Asagoshi,‡ Hiroaki Odawara,‡ Hironobu Nakano,‡ Takayuki Miyano,‡ Hiroaki Terato,‡ Yoshihiko Ohyama,‡ Shuji Seki,§,|| and Hiroshi Ide*,‡

Department of Mathematical and Life Sciences, Graduate School of Science, Hiroshima University, Higashi-Hiroshima 739-8526, Japan, and Institute of Cellular and Molecular Biology, Okayama University Medical School, Okayama 700-8558, Japan

Received February 23, 2000; Revised Manuscript Received May 31, 2000

ABSTRACT: *Escherichia coli* endonuclease III (Endo III) and its eukaryotic homologues are major repair enzymes for pyrimidine lesions formed by reactive oxygen species and ionizing radiation. In the present study, the activities of Endo III and its mouse homologue (mNTH1) have been compared using defined oligonucleotide substrates containing a urea residue (UR), two *cis*-thymine glycol (TG) diastereoisomers, 5,6-dihydrothymine (DHT), and 5-hydroxyuracil (HOU). The substrates were incubated with Endo III and mNTH1, and their activities were compared based on the product analysis by gel electrophoresis. Endo III recognized all base lesions tested, but the activity for DHT was extremely lower than other substrates. In contrast, albeit some preference of UR, mNTH1 showed essentially comparable activities for all substrates including DHT. Comparison of the enzymatic parameters for *cis*-TG and DHT revealed that large decreases in the affinity (K_m, 27-fold) and k_{cat} (11-fold) relative to *cis*-TG made DHT an very poor substrate for Endo III. mNTH1 had comparable affinities and k_{cat} for both *cis*-TG and DHT, though turnover (k_{cat}) of mNTH1 was notably slower than Endo III. In view of the reaction mechanism, the paired base effect on the damage recognition by the two enzymes was also examined. The activities of Endo III for UR and HOU were paired base-independent, but those for *cis*-TG and DHT were significantly enhanced when paired with G. With mNTH1, the paired base effect was evident only for DHT. The variations of the repair activity with paired bases and enzymes are discussed in relation to the base flipping mechanism suggested for base excision repair enzymes.

Damage to DNA caused by reactive oxygen species is one of the most frequent genetic lesions encountered in living cells (*1*, *2*). It becomes increasingly important to understand how cells deal with such oxidative DNA damage in light of their possible link to carcinogenesis and aging (*3*−*5*). Oxidative base damage blocks DNA synthesis and/or directs misincorporation of nucleotides depending on the lesion structure during DNA replication, hence lethal and/or mutagenic (reviewed in ref *6*). To avoid such cytotoxic and mutagenic effects, oxidative base lesions are removed by repair enzymes mostly through the base excision repair (BER)[1] pathway in prokaryotic and eukaryotic cells (*7*). Endonuclease (Endo) III involved in the BER pathway in *Escherichia coli* shows a broad substrate specificity, excising a number of pyrimidine lesions formed by reactive oxygen species and ionizing radiation (*6*−*8*). Endo III encoded by the *nth* gene (*9*, *10*) is a monomeric protein with a molecular mass of 23.4 kDa and acts as *N*-glycosylase/AP lyase (*11*, *12*). This enzyme contains the helix−hairpin−helix (HhH) motif essential for the activity and the 4Fe-4S cluster for DNA binding (*13*−*15*). The *nth* mutant of *E. coli* exhibits only weak mutator phenotype and is not particularly sensitive to X-rays or hydrogen peroxide (*9*). However, the *nth nei* double mutant lacking both Endo III and Endo VIII (the *nei* gene product) exhibits spontaneous mutator phenotype and is sensitive to X-rays and hydrogen peroxide (*16*, *17*), suggesting redundant repair pathways for oxidized pyrimidine lesions.

Recently, the genes of eukaryotic Endo III homologues have been cloned from several sources including *Saccharomyces serevisiae* (*18*, *19*), *Schizosaccharomyces pombe* (*20*), mouse (*21*), and human (*22*, *23*). These enzymes contain the DNA recognition HhH motif, two key amino acids (corresponding to Lys-120 and Asp-138 in Endo III) essential for catalysis, and the 4Fe-4S cluster (except NTG1 of *S. serevisiae*). Although *S. serevisiae* homologues (NTG1 and NTG2) have an additional activity for formamidopyrimidine, all of the expressed proteins of yeast (*18*−*20*, *24*, *25*), mouse (*21*), and human (*22*, *23*, *26*) exhibit substrate specificity similar to that of Endo III when the activity is assayed using

† This work was supported by grants-in-aid from the Ministry of Education, Science, and Culture of Japan (to H.I.).

* To whom correspondence should be addressed at the Department of Mathematical and Life Sciences, Graduate School of Science, Hiroshima University, Higashi-Hiroshima 739-8526, Japan. Phone & Fax: +81-824-24-7457. E-mail: ideh@hiroshima-u.ac.jp.

‡ Hiroshima University.

§ Okayama University Medical School.

|| Present address: Department of Human Nutrition, Chugoku Junior College, 83 Niwase, Okayama 701-0197, Japan.

[1] Abbreviations: BER, base excision repair; Endo, endonuclease; NTG1(2), endonuclease III-like glycosylase 1(2); m(h)NTH1, mouse (human) endonuclease III homologue; HhH, helix−hairpin−helix; TG, thymine glycol; DHT, 5,6-dihydrothymine; UR, urea residue; HOU, 5-hydroxyuracil; dTG, thymidine glycol; DHdT, 5,6-dihydrothymidine; PAGE, polyacrylamide gel electrophoresis.

10.1021/bi000422l CCC: $19.00
Published on Web 08/19/2000

Table 1: List of Oligonucleotides Used in This Study

abbreviation	sequence[a]
19T	5′-ACAGACGCCAT̲CAACCAGG
19UR	5′-ACAGACGCCAW̲CAACCAGG
19TG1	5′-ACAGACGCCAX̲CAACCAGG
19TG2	5′-ACAGACGCCAY̲CAACCAGG
19DHT	5′-ACAGACGCCAD̲CAACCAGG
19HOU	5′-ACAGACGCCAZ̲CAACCAGG
19COM-A	3′-TGTCTGCGGTA̲GTTGGTCC
19COM-G	3′-TGTCTGCGGTG̲GTTGGTCC
19COM-C	3′-TGTCTGCGGTC̲GTTGGTCC
19COM-T	3′-TGTCTGCGGTT̲GTTGGTCC

[a] W = UR, X = *5S,6R*-TG, Y = *5R,6S*-TG, D = DHT, Z = HOU.

oligonucleotides or DNA containing defined lesions as substrates. However, comparison of the activities of Endo III (*27*) and its yeast (*28*, *29*) and human (*30*) homologues using γ-irradiated DNA suggests significant differences in the substrate specificity and excision kinetics of these enzymes.

In view of the apparent discrepancies of the repair activity of Endo III and its eukaryotic homologues described above, we felt it was important to compare their activity for different substrates on a quantitative basis. In the present study, five pyrimidine lesions [two diastereoisomers of *cis*-thymine glycol (TG), 5,6-dihydrothymine (DHT), 5-hydroxyuracil (HOU), and a urea residue (UR)] were site-specifically-incorporated into synthetic oligonucleotides and the relative activities of Endo III and its mouse homologue (mNTH1) toward these lesions were compared.

EXPERIMENTAL PROCEDURES

Enzymes. *Penicillium citrinum* nuclease P1, *Crotulus durissus* phosphodiesterase, and calf intestine alkaline phosphatase were purchased from Boehringer Mannheim, and T4 polynucleotide kinase was from New England Biolabs. Endo III was purified from *E. coli* cells overexpressing the *nth* gene product (a gift from Wallace and Hatahet) (*31*). The cloned mouse Endo III homologue (mNTH1/mNTHL1) was overproduced in the *nth nei* mutant of *E. coli* and purified as described previously (*21*). In the expressed mNTH1 protein, the N-terminal amino acid (M) was replaced by an oligopeptide ($MRGSH_6G_2TEF$) for affinity purification. Both Endo III and mNTH1 exhibited a single protein band in SDS−PAGE analysis. The protein concentration of Endo III and mNTH1 was determined by the BCA protein assay reagent kit (Pierce) with bovine serum albumin (BSA) as the standard.

Oligonucleotides. Oligonucleotides used in this work are listed in Table 1. 19T and its complementary strands [19COM-N (N = A, G, C, T)] were synthesized by the standard phosphoramidite method and purified by reversed phase HPLC. 19DHT and 19HOU containing DHT and HOU, respectively, were synthesized using β-cyanoethyl phosphoramidite monomers of DHT and HOU (Glen Research) in combination with phenoxyacetyl (Pac) protected dA, 4-isopropyl-phenoxyacetyl (^{i}Pr-Pac) protected dG, and acetyl protected dC as normal components. Deprotection of 19DHT and 19HOU was performed under mild conditions (50 mM K_2CO_3 in methanol at room temperature for 2 h) to avoid decomposition of incorporated DHT and HOU. 19DHT and 19HOU were purified by reversed phase HPLC. 19TG1 and 19TG2 containing *5S,6R*-TG and *5R,6S*-TG diastereoisomers, respectively, were prepared by $KMnO_4$ oxidation of 19T following the reported method (*32*) with modifications. It is known that $KMnO_4$ oxidation of thymidine (dT) gives rise to two diastereoisomers of *cis*-thymidine glycol (dTG) with *5R,6S*-dTG as a major product and *5S,6R*-dTG as a minor product (*32*, *33*). 19T (12 OD) was dissolved in 140 mM phosphate buffer (pH 8.6, 340 μL), and the solution was kept on ice for 10 min. $KMnO_4$ (final concentration 12 mM) was added to the solution, and the solution was stirred on ice for 2 min. The reaction was terminated by addition of allyl alcohol (24 μL), and precipitated MnO_2 was removed by centrifugation. Crude products were mixed with water (1 mL) and loaded onto a C18 Sep-Pak cartridge (1 mL, Waters). The cartridge was washed with water (2 mL), and oligonucleotides were eluted by acetonitrile/water [6:4 (v/v), 2 mL]. After evaporation, oligonucleotides were suspended in a small volume of water and purified by HPLC. The HPLC system consisted of Jasco PU-980 pumps equipped with a C18 WS-DNA column (10 × 250 mm for preparative use, 4.6 × 150 mm for analytical use, Wako), a UV-975 detector (monitoring wavelength 260 nm), and an 807-IT integrator. Samples were eluted by a linear gradient of acetonitrile (7−12%) in 0.1 M triethylammonium acetate (TEAA, pH 7.0) with a flow rate of 2 mL/min (preparative column) or 0.8 mL/min (analytical column). The oligonucleotides containing *5R,6S*- and *5S,6R*-isomers of *cis*-TG (19TG2 and 19TG1, respectively) were eluted as the major and the second major product peaks (Figure 1A). HPLC separation of oligonucleotides containing diastereoisomers of the base unit or the internucleotide linkage has been reported in previous studies (e.g., *34*−*36*), where the HPLC conditions were essentially similar to those of the present study. The fractions containing 19TG1 and 19TG2 were collected, evaporated, and used for the experiments. The analytical HPLC profiles of 19TG1 and 19TG2 are shown in Figures 1B and 1C, respectively. The nucleosides present in 19TG1 and 19TG2 were analyzed by nuclease/alkaline phosphatase digestion. Surprisingly, single nuclease digestion (phosphodiesterase or nuclease P1) of 19TG2 followed by alkaline phosphatase treatment did not result in the expected peak of *cis*-dTG in HPLC analysis. Instead, peaks of unknown products were detected together with those of dA, dG, and dC. Comparison of the retention time of $KMnO_4$-oxidized AT and TC dimers containing *cis*-TG isomers (t′) suggested that the unknown products formed by phosphodiesterase were At′ dimers, whereas those by nuclease P1 were t′C dimers. Thus, dimers containing 3′- and 5′-*cis*-TG isomers were resistant to phosphodiesterase and nuclease P1, respectively. Distinctive activities of phosphodiesterase and nuclease P1 to dimers containing a 5′- or 3′-abasic site have been reported previously (*37*), and the influences of the 3′- and 5′-abasic site regarding the resistance to these nucleases are similar to those of *cis*-TG. For complete digestion, 19TG2 was subjected to double digestion by phosphodiesterase and nuclease P1 with different substrate specificities. HPLC analysis of the digested products (i.e., nucleosides) was performed as described above except that the monitoring wavelength was set at 210 nm and the eluent was 5% methanol in 10 mM phosphate buffer (pH 7.4). The results clearly demonstrated the presence of *cis*-dTG (retention time

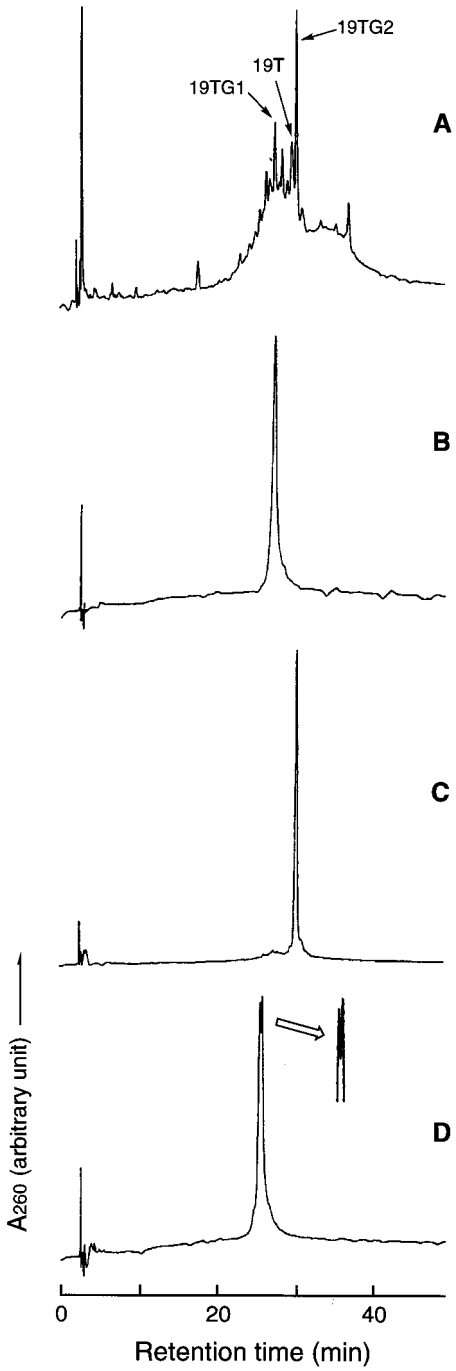

FIGURE 1: HPLC elution profiles of $KMnO_4$-treated 19T, and purified 19TG1, 19TG2, and 19UR. The sample was separated on a C18 WS-DNA column (4.6 × 150 mm) using a gradient of acetonitrile (7−12%) in 0.1 M TEAA buffer (pH 7.0). The monitoring wavelength was 260 nm. (A) Reaction mixture obtained by $KMnO_4$ treatment of 19T, (B) 19TG1, (C) 19TG2, and (D) 19UR.

5.7 min) and the absence of dT that was present in the digested product of 19T (retention time 23.0 min) (Figure 2A,C). HPLC analysis of the reaction products by double nuclease digestion of 19TG1 showed a chromatograph essentially similar to that of 19TG2, indicating the presence of *cis*-dTG and the absence of dT in 19TG1 (Figure 2B). Since the two diastereoisomers of authentic *cis*-dTG (prepared by $KMnO_4$ oxidation of dT) were not separated under the present HPLC conditions, we concluded that 19TG1, the second major product of 19T oxidation, contained the minor *5S,6R*-isomer of TG. In contrast to 19TG1 and 19TG2, 19DHT containing DHT was readily digested by a single nuclease (phosphodiesterase or nuclease P1), yielding the HPLC peak of *5S*-dihydrothymine (DHdT). The peak of the *5R*-diastereoisomer of DHdT was obscured by the overlapping dG peak (Figure 2D). The authentic samples of *5S*- and *5R*-DHdT were provided by S. Nishimoto (Kyoto University).

19UR was prepared by alkali treatment of 19TG2 (*38*). 19TG2 in a microdialysis cup was dialyzed against 40 mM phosphate buffer (pH 12) containing 2 mM EDTA at room temperature overnight. The solution was dialyzed against 10 mM Tris-HCl (pH 7.5), 1 mM EDTA at 4 °C (8 h × 2), and then water (8 h × 2). Finally, 19UR was purified by HPLC as described for 19TG2. 19UR prepared by alkali treatment of 19TG2 showed characteristic doublet peaks that were well separated from 19TG1 in HPLC analysis (Figure 1D). The alkali treatment of 19TG1 also yielded the same doublet peaks (not shown). Incorporation of a urea residue into oligonucleotides using the phosphoramidite monomer of 2′-deoxyribosylurea has been reported previously (*39*, *40*). The oligonucleotide prepared by this method was also eluted as two separated peaks in the reversed phase HPLC (*40*). The NMR study of the separated oligonucleotides has revealed that they contain the urea side chain existing in different conformations (*39*, *40*). Accordingly, the present HPLC data on 19UR prepared by alkali treatment of 19TG2 (or 19TG1) were consistent with the reported studies. 19TG1 and 19TG2 were incised at the TG site by Endo III but not Endo IV or exonuclease III, whereas 19UR were incised by all three enzymes (data not shown). These results were consistent with the known substrate specificity of the enzymes (*6*−*8*).

Activity Assay of Endo III and mNTH1. 19UR, 19TG1, 19TG2, 19DHT, and 19HOU were 5′-end-labeled with [γ-^{32}P]ATP (110 Tbq/mmol, Amersham Pharmacia) and T4 polynucleotide kinase, and purified as described (*41*). The oligonucleotides were annealed to 19COM-A (19UR, 19TG1, 19TG2, 19DHT) or 19COM-G (19HOU, HOU is a damage derived from C). The constructed duplexes (10 nM) were incubated with Endo III [1 ng (4 nM) or 20 ng (86 nM)] or mNTH1 [5 ng (15 nM)] in appropriate buffer (10 μL) at 37 °C for 10 min (Endo III) or 30 min (mNTH1). The composition of Endo III buffer was 10 mM Tris-HCl (pH 7.5), 100 mM NaCl, 1 mM EDTA, and that of mNTH1 was 20 mM HEPES−KOH (pH 8.0), 50 mM KCl, 0.25 mM EDTA, 0.25 mM dithiothreitol, 0.1 mg/mL BSA. For the time course study on product formation, the substrates were treated by Endo III and mNTH1 as described above except that the incubation time was varied for up to 20 min (Endo III) and 90 min (mNTH1). The enzymatic parameters of Endo III and mNTH1 for *cis*-TG and DHT (both paired with A) were also obtained in essentially similar manners. The concentration range of the substrate was 1−50 nM for 19TG2 (Endo III and mNTH1), 10−600 nM for 19DHT (Endo III), and 1−50 nM for 19DHT (mNTH1). The amount of Endo III was 0.5 ng (2 nM) for 19TG2 or 20 ng (86 nM) for 19DHT, and that of mNTH1 was 3 ng (9 nM) for 19TG2 and 19DHT. The incubation time was 5 or 10 min depending on the combination of the substrate and enzyme. Products were analyzed by PAGE as described below. The enzymatic parameters (K_m and k_{cat}) were evaluated from $S-V$ plots using a hyperbolic curve-fitting program. The parameters of Endo

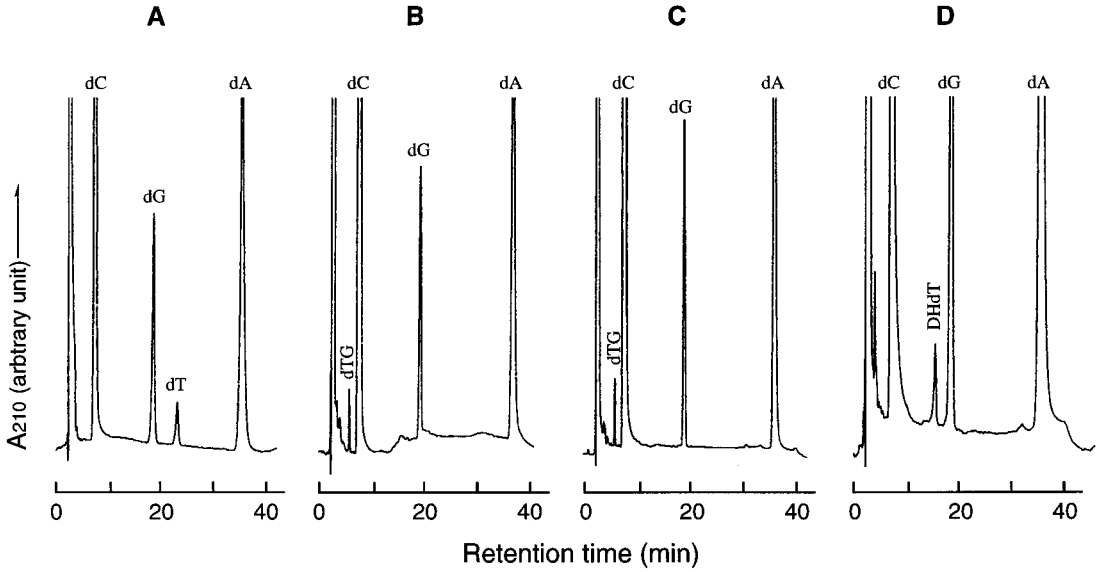

FIGURE 2: HPLC analysis of the nucleosides from enzymatic digestion of 19T, 19TG1, 19TG2, and 19DHT. 19T, 19TG1, and 19TG2 were digested by nuclease P1 and phosphodiesterase simultaneously, and the resulting nucleoside monophosphates were further dephosphorylated by alkaline phosphatase. 19DHT was digested by nuclease P1 and subjected to alkaline phosphatase treatment. The sample was separated on a C18 WS-DNA column (4.6 × 150 mm) using 5% methanol in 10 mM phosphate buffer (pH 7.4). The monitoring wavelength was 210 nm. The HPLC profiles are for the digested products of (A) 19T, (B) 19TG1, (C) 19TG2, and (D) 19DHT. In chromatogram D, the peak of *5R*-DHdT was obscured by the overlapping dG peak, and only the peak of *5S*-DHdT was observed.

III for the substrates containing mispairs of TG:G (19TG2/19COM-G) and DHT:G (19DHT/19COM-G) were determined as described above except that the amount of the enzyme was reduced to one-fourth. In the experiments to determine paired base effects, 19UR, 19TG2, 19DHT, and 19HOU were annealed to 19COM-N (N = A, G, C, and T). The substrates containing four possible pairs (5 nM) were incubated with Endo III [0.5 ng (2 nM) or 10 ng (43 nM)] or mNTH1 [3 ng (9 nM)] at 37 °C for 5 or 10 min.

Product Analysis by PAGE. After enzymatic treatments of the oligonucleotide substrates, the sample was mixed with gel loading buffer (0.05% xylene cyanol, 0.05% bromophenol blue, 20 mM EDTA, and 98% formamide), heat-denatured, and separated by 16% denaturing PAGE. The gel was autographed at −80 °C overnight. Alternatively, the radioactivity of the separated band was analyzed by Fuji BAS 2000.

Cross-Link Reaction with $NaBH_4$. To analyze the reaction intermediates, the duplex substrates [19TG1, 19TG2, 19DHT, 19UR (all annealed to 19COM-A), 3 nM] in Endo III or mNTH1 buffer (10 μL) were incubated with Endo III [10 ng (43 nM) or mNTH1 [20 ng (58 nM)] in the presence or absence of 50 mM $NaBH_4$ at 37 °C for 30 min. After incubation, the sample was mixed with SDS-loading buffer [100 mM Tris, 8% SDS, 24% (v/v) glycerol, 4% 2-mercaptoethanol, 0.02% SERVA Blue G] and heat-denatured. The sample was separated by 10% SDS−polyacrylamide gel electrophoresis (SDS−PAGE). Autoradiography was performed as described above. The fraction of active Endo III and mNTH1 used in the experiments was also estimated by the $NaBH_4$-trapping assay. 19TG2/19COM-A (25−300 nM) was incubated with Endo III [23 ng (100 nM)] or mNTH1 [34 ng (100 nM)] in the presence of $NaBH_4$ as described above, and the free and cross-linked substrates were quantitated by SDS−PAGE analysis. The fraction of the active enzyme was estimated as the maximum amount of the trapped enzyme−substrate complex.

RESULTS

Substrate Specificities of Endo III and mNTH1. The activities of Endo III and mNTH1 to pyrimidine lesions were examined using oligonucleotide substrates in which UR (19UR), *5S,6R*-TG (19TG1), *5R,6S*-TG (19TG2), and HOU (19HOU) were embedded in the same site (Table 1). The oligonucleotides were annealed to 19COM-G (19HOU) or 19COM-A (other substrates), and the duplex substrates were incubated with Endo III or mNTH1. Products were analyzed by PAGE (Figure 3). All pyrimidine lesions were recognized by both Endo III and mNTH1 so that specific incision products were observed in the PAGE analysis. The β-elimination products formed by Endo III migrated as doublet bands (Figure 3A) probably due to different 3′-terminal deoxyribose modifications, i.e., Tris adducts or isomers of hydroxypentenal termini (*42*−*44*), while those by mNTH1 showed a single band corresponding to the fast migrating product by Endo III (Figure 3B). It should be noted that the activity of Endo III to 19DHT was very low relative to other substrates so that a large excess of Endo III was required to achieve nicking comparable to other substrates (Figure 3A, lanes 8 and 9). However, this was not the case for mNTH1 (Figure 3B, lane 8).

To compare the substrate specificity of Endo III and mNTH1 quantitatively, the amount of nicked substrate was quantified based on the product analysis by PAGE. Typical time course plots of the product formation by Endo III and mNTH1 are shown in Figures 4A and 4B, respectively. The substrate specificities of the enzymes were compared based on the amount of products formed at the fixed incubation time (10 min for Endo III and 30 min for mNTH1). These results are shown in Figures 5A (Endo III) and 5B (mNTH1). UR, two *cis*-TG isomers, and HOU were good substrates of Endo III, and the activities for these substrates were essentially comparable. In contrast, DHT was an extremely poor substrate of Endo III. The activity for DHT was roughly

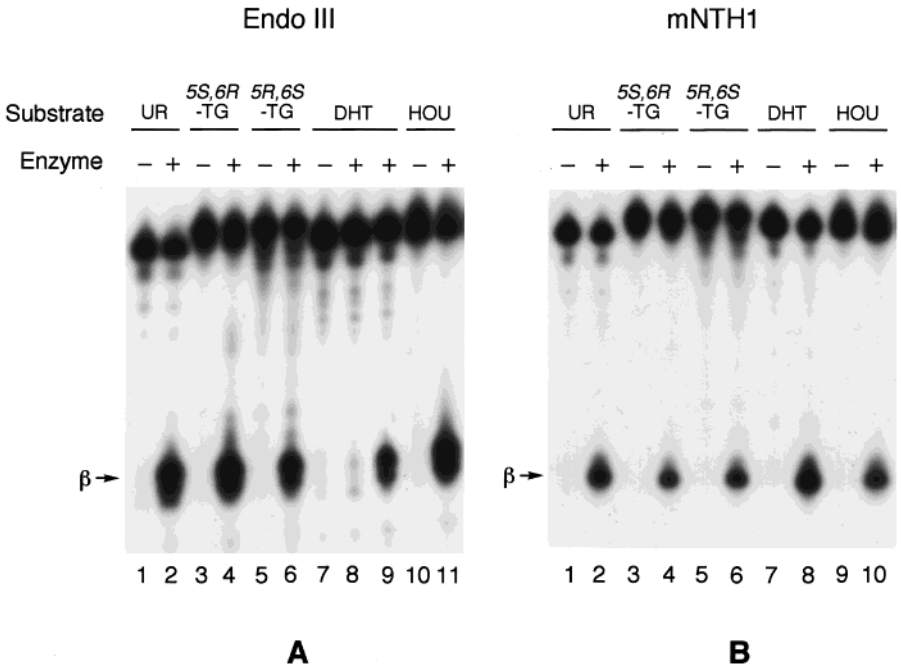

FIGURE 3: PAGE analysis of the reaction products formed by Endo III and mNTH1. (A) 19UR (containing UR), 19TG1 (*5S,6R*-TG), 19TG2 (*5R,6S*-TG), and 19DHT (DHT) were annealed to 19COM-A, and 19HOU (HOU) to 19COM-G. The substrates (10 nM) were treated with Endo III [1 ng (4 nM) in lanes 2, 4, 6, 8, 11 and 20 ng (86 nM) in lane 9] for 10 min, and products were analyzed by 16% PAGE as described under Experimental Procedures. (B) The same substrates were treated with mNTH1 [5 ng (15 nM) in lanes 2, 4, 6, 8, 10] for 30 min. β-Elimination products are indicated by the arrow.

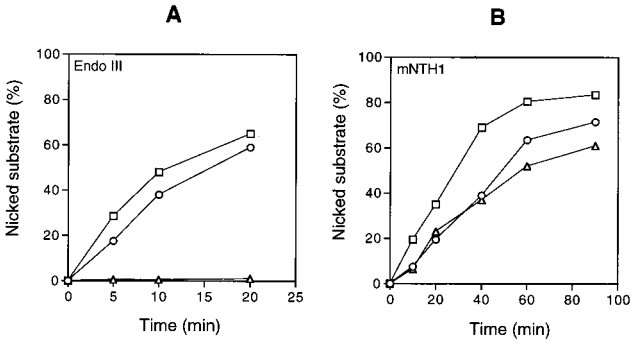

FIGURE 4: Typical time course plots of product formation by Endo III and mNTH1. 19UR, 19TG2, and 19DHT were annealed to 19COM-A, and the substrates (10 nM) were incubated with Endo III [1 ng (4 nM)] or mNTH1 [5 ng (15 nM)] for the indicated time. Products were analyzed by 16% PAGE. The percent of nicked substrates was plotted against incubation time. (□) 19UR, (○) 19TG2, (△) 19DHT.

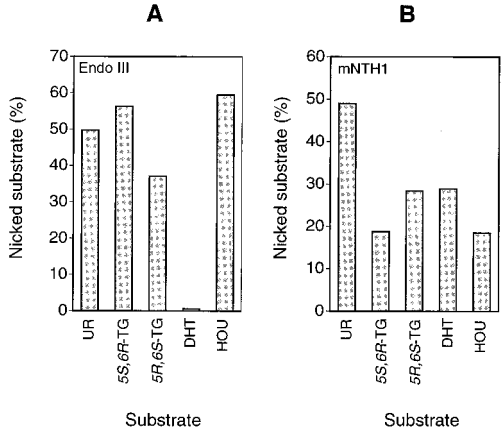

FIGURE 5: Comparison of the activities of Endo III and mNTH1 to pyrimidine lesions. The substrates (10 nM) containing UR, *5S,6R*-TG, *5R,6S*-TG, DHT, and HOU were incubated with (A) Endo III [1 ng (4 nM)] for 10 min or (B) mNTH1 [5 ng (15 nM)] for 30 min, and the percentage of nicked substrates was determined by PAGE analysis as shown in Figure 3. The percentage of nicked products (average of three independent experiments) was plotted against the pyrimidine lesions.

100-fold lower than other substrates. mNTH1 recognized all pyrimidine lesions with some preference of UR. DHT was efficiently recognized by mNTH1, and the activity to DHT was comparable to *cis*-TG and HOU.

To delineate the reaction mechanism responsible for the large difference in the relative activity to DHT between Endo III and mNTH1, enzymatic parameters for DHT and *cis*-TG were determined and compared (Table 2). According to the K_m values, the apparent affinity of Endo III for the substrate containing DHT (K_m = 510 nM) was 27-fold lower than that for *cis*-TG (=19 nM). Similarly, k_{cat} for DHT (=0.07 min^{-1}) was 11-fold lower than that for *cis*-TG (=0.78 min^{-1}). Thus, the combined effects of the low affinity and k_{cat} made DHT an extremely poor substrate for Endo III, with the k_{cat}/K_m ratio being 1:315 for DHT vs *cis*-TG. mNTH1 showed comparable affinities (K_m) and k_{cat} for DHT and *cis*-TG, although the turnover rates (k_{cat}) of mNTH1 were notably lower than those of Endo III. As a result, k_{cat}/K_m of mNTH1 for DHT was virtually comparable to that for *cis*-TG (DHT:TG = 0.66:1).

Table 2: Comparison of Enzymatic Parameters of Endo III and mNTH1 for *cis*-TG and DHT[a]

enzyme	substrate	K_m (nM)	k_{cat} (min^{-1})	k_{cat}/K_m ($\times 10^4$)
Endo III	TG:A[b]	19	0.78	410
	DHT:A	510	0.07	1.3
	TG:G[b]	6	0.79	1300
	DHT:G	62	0.15	24
mNTH1	TG:A[b]	3	0.03	100
	DHT:A	3	0.02	66

[a] Average of two independent experiments. [b] TG = *5R,6S*-TG.

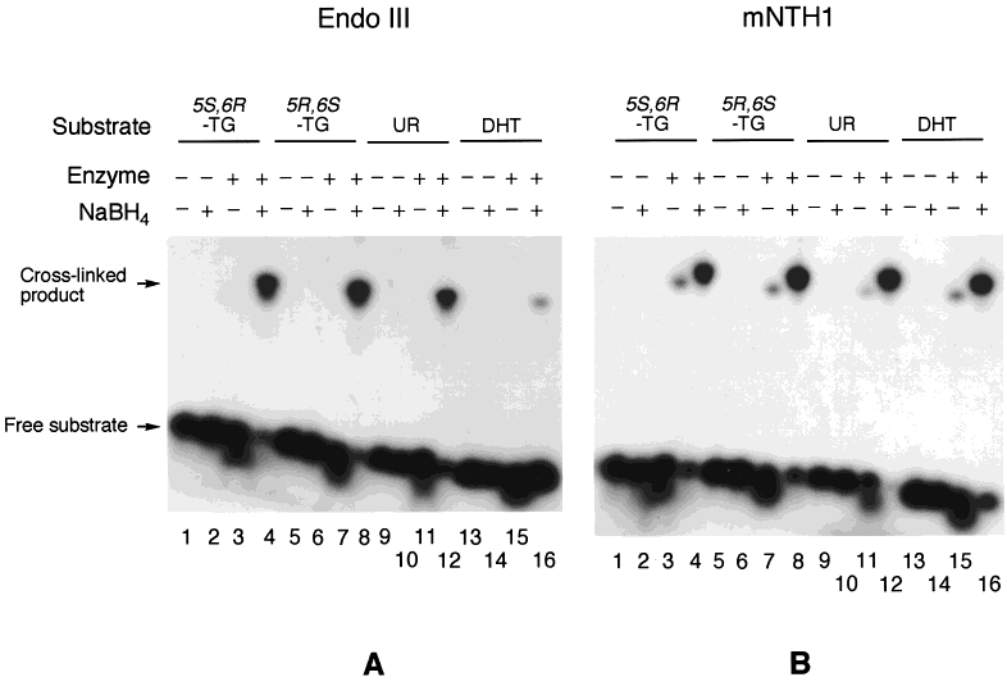

FIGURE 6: $NaBH_4$-trapping of the Schiff base intermediates. 19UR (containing UR), 19TG1 (*5S,6R*-TG), 19TG2 (*5R,6S*-TG), and 19DHT (DHT) were annealed to 19COM-A. The duplex substrates (3 nM) were incubated with (A) Endo III [10 ng (43 nM)] or (B) mNTH1 [20 ng (58 nM)] in the presence and absence of 50 mM $NaBH_4$. Cross-linked products were analyzed by 10% SDS−PAGE. Treatments without (shown by −) and with (+) enzyme or $NaBH_4$ are indicated on the top of the gel together with the substrates. The cross-linked products and free substrates are indicated by arrows.

$NaBH_4$-Trapping Assay of the Schiff Base Intermediates. Comparison of the substrate specificity of Endo III and mNTH1 (Figure 5 and Table 2) revealed that UR, *cis*-TG isomers, and HOU were comparable substrates, while DHT was differentially recognized by Endo III and mNTH1. The Endo III superfamily is known to form the Schiff base intermediate, which can be trapped (or irreversibly cross-linked) by $NaBH_4$ or $NaBH_3CN$ reduction (reviewed in ref *8*). Therefore, the amount of the trapped Schiff base intermediate provides another measure of the substrate specificity of Endo III and mNTH1. The duplex substrates containing UR, *cis*-TG isomers, and DHT were incubated with Endo III or mNTH1 in the presence and absence of $NaBH_4$, and products were analyzed by SDS−PAGE (Figure 6). Incubation of 19TG1, 19TG2, and 19UR (Figure 6A, lanes 4, 8, 12) resulted in strong shifted bands indicative of the trapped Schiff base intermediates, but the corresponding band formed with 19DHT was much weaker (lane 16). The trapping experiments with mNTH1 resulted in similar shifted bands with a comparable intensity for all substrates including 19DHT (Figure 6B, lanes 4, 8, 12, 16). Thus, the amount of trapped Schiff base intermediates for Endo III and mNTH1 paralleled the substrate specificity obtained by the analysis of incision products (Figure 5). Interestingly, incubation with mNTH1 in the absence of $NaBH_4$ also gave rise to weak shifted bands (Figure 6B, lanes 3, 7, 11, 15), and the gel mobilities of the bands were comparable to those of the cross-linked DNA/mNTH1 complexes by $NaBH_4$ (lanes 4, 8, 12, 16). Such bands were not observed for Endo III in the treatment without $NaBH_4$. These bands were tentatively assigned as reaction intermediates (Schiff base) based on their gel mobilities. It is possible that formation of a stable reaction intermediate for mNTH1 slows down turnover of this enzyme, thereby resulting not only in the reduction of k_{cat} relative to Endo III (Table 2) but also in the apparent inhibition of the enzyme.

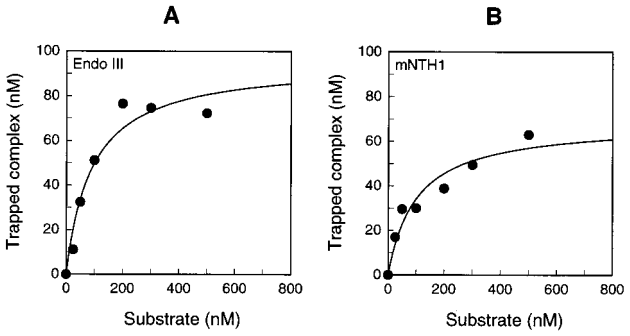

FIGURE 7: Estimation of the fraction of active Endo III and mNTH1 by the $NaBH_4$-trapping assay. 19TG2/19COM-A with the indicated concentration was incubated with (A) Endo III [23 ng (100 nM)] or (B) mNTH1 [34 ng (100 nM)] in the presence of 50 mM $NaBH_4$ at 37 °C for 30 min, and the free substrate and the trapped complex were quantitated by SDS−PAGE analysis. The concentration of the trapped complex (Schiff base) was plotted against that of the substrate. The fraction of the active enzyme was evaluated as the maximum concentration of the trapped complex by hyperbolically extrapolating the experimental data (solid curve) to the value at infinite concentration of the substrate.

Figure 7 shows the results of the $NaBH_4$-trapping assay to estimate the fraction of active Endo III and mNTH1. In the experiments, the concentration of the enzyme (Endo III and mNTH1) was fixed (100 nM), and that of the substrate (19TG2/19COM-A) was varied up to 500 nM. The concentration of the trapped complex was determined based on the ratio of the amounts of free and cross-linked substrates, and plotted against the concentration of the substrate. The fraction of the active enzyme was evaluated as the maximum concentration of the trapped complex by hyperbolically extrapolating the experimental data to the value at the infinite concentration of the substrate. The maximum concentration

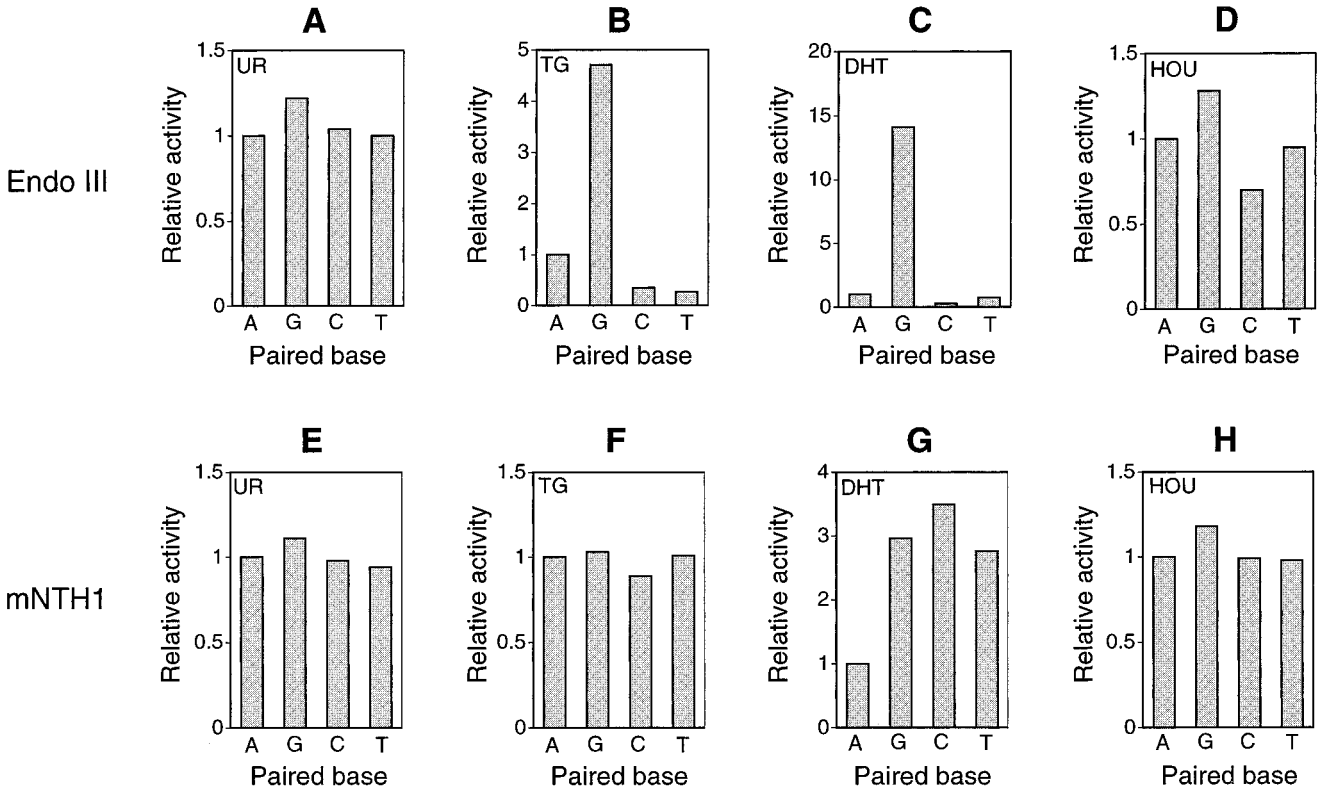

FIGURE 8: Paired base effects on the repair activity of Endo III and mNTH1. 19UR (containing UR), 19TG2 (*5R,6S*-TG), 19DHT (DHT), and 19HOU (HOU) were annealed to four complementary strands [19COM-N (N = A, G, C, T)]. The substrates (5 nM) were incubated with Endo III [0.5 ng (2 nM) for UR, TG, HOU or 10 ng (43 nM) for DHT] or mNTH1 [3 ng (9 nM)]. The activities determined by PAGE analysis were standardized relative to that for the base pair containing A for each base lesion. The data were the average of three independent experiments. (A) UR, (B) *5R,6S*-TG, (C) DHT, (D) HOU with Endo III; and (E) UR, (F) *5R,6S*-TG, (G) DHT, (H) HOU with mNTH1.

of the trapped complex was 95 nM for Endo III and 68 nM for mNTH1, indicating that Endo III and mNTH1 used in the present study were 95% and 68% active, respectively. These values are regarded as the minimum values of the active fraction since inactivation of the enzymes during the trapping reaction was not taken into consideration. In view of the fact that the fractions of active Endo III and mNTH1 were reasonably high and approximately comparable, the k_{cat} values obtained for the enzymes (Table 2) were not corrected by the factor of the active fraction.

Paired Base Effects on the Repair Activity of Endo III and mNTH1. It has been suggested that Endo III uses a base flipping mechanism for excision of aberrant bases (*14*). Accordingly, it may be possible that a base opposite the lesion alters the geometry or disposition of the base pair and affects the extrusion process of an aberrant base. To examine the influence of the paired base, the substrates containing four possible base pairs (A, G, C, T) were constructed for each lesion (UR, *cis*-TG, DHT, and HOU), and the repair activities of Endo III and mNTH1 were determined. The variation of the repair activity with paired bases is shown in Figure 8, where the activity for each damage was standardized relative to that for the pair containing A as an opposite base. With Endo III (Figure 8A−D), the activities for UR and HOU were essentially independent of the paired base, whereas those for *cis*-TG and DHT were significantly affected, with a preference of G. The activity for TG:G and DHT:G pairs increased by 4.7- and 14-fold, respectively, in comparison with those paired with A. The preference of TG:G and DHT:G pairs over those paired with A was further substantiated by the analysis of enzymatic parameters (Table 2). The k_{cat}/K_m values for TG:G and DHT:G pairs were greater than TG:A and DHT:A pairs by 3- and 18-fold, respectively. The increase in the activity primarily originated from increased affinity (K_m) for TG:G (3-fold) and DHT:G (8-fold). Similar to Endo III, the activities of mNTH1 for UR and HOU were essentially independent of the paired base (Figure 8E,H), but unlike Endo III, that for *cis*-TG was also virtually paired base-independent (Figure 8F). A DHT:G pair was a preferred substrate over a DHT:A pair (3-fold). In addition, DHT paired with pyrimidines (C and T) was also excised with an efficiency comparable to a DHT:G pair.

DISCUSSION

In the present study, substrate specificities of Endo III and mNTH1 were compared using five different pyrimidine lesions. Two diastereoisomers of *cis*-TG were recognized by Endo III and mNTH1 with comparable efficiencies (Figure 5). To our knowledge, this study is the first report on the comparison of the activity of DNA repair enzymes to the diastereoisomers of *cis*-TG. Unlike $KMnO_4$ oxidation of DNA that favors the formation of *5R,6S*-TG over *5S,6R*-TG, ionizing radiation generates essentially equal amounts of the two diastereoisomers in DNA (*45*). Since Endo III and mNTH1 recognized both isomers, it may be reasonable to predict that the two *cis*-TG diastereoisomers present in irradiated DNA will be excised with comparable rates in cells. The *cis*-TG isomers bear two hydroxyl groups projecting opposite sides of the pyrimidine ring. However, the orientation of the hydroxyl groups relative to the pyrimidine ring did not affect the substrate recognition of Endo III and mNTH1, hence ruling out the specific interaction between

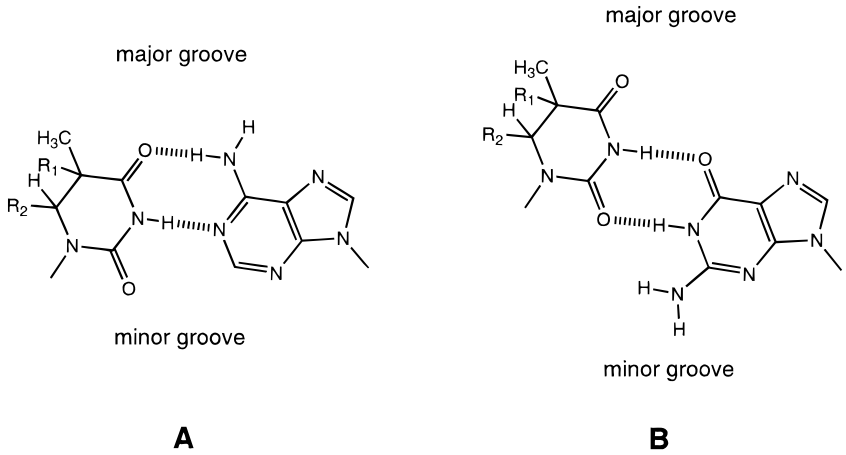

FIGURE 9: Possible base pairing schemes of TG and DHT with A and G. (A) A Watson−Crick base pair (paired with A) and (B) a wobble base pair (paired with G). Putative hydrogen bonds are shown by broken lines. In the pyrimidine structure, R_1 and R_2 = OH for TG and R_1 and R_2 = H for DHT.

the hydroxyl groups and the enzymes in damage recognition. This notion is also consistent with the wide substrate specificities of Endo III and mNTH1 that accept a variety of pyrimidine lesions with no apparent structural similarities (*6*−*8*).

An intriguing result with respect to the substrate specificity of Endo III and mNTH1 was the activity difference to DHT. Although mNTH1 had apparently lower turnover rates than Endo III (Table 2), the specificity constant (k_{cat}/K_m) indicates that *cis*-TG and DHT are comparable substrates of mNTH1 but not Endo III. These results were further confirmed by the analysis of the Schiff base intermediate formed between the enzymes and substrates (Figure 6). The substrate specificity of eukaryotic Endo III homologues such as those from human (hNTH1) and *S. serevisiae* (NTG1 and NTG2) has been studied using γ-irradiated DNA as a substrate. Although this substrate contains similar amounts of TG, DHT, and HOU (TG:DHT:HOU = 1.31:0.46:1.42) (*29*), hNTH1 excised only TG but not DHT and HOU (*30*). NTG1 and NTG2 excised TG and HOU but not DHT (*29*). A weak activity of NTG1 and NTG2 to DHT relative to *cis*-TG in oligonucleotides was also implicated recently though quantitative comparison was not made (*46*). In the present study, mNTH1 was shown to recognize DHT and HOU as well as TG that was the only substrate recognized by hNTH1 in the three pyrimidine lesions. The amino acid sequence is highly conserved between mNTH1 and hNTH1 (81% identical), but there are some variations (*21*). It is not clear whether such variations of amino acids account for the discrepancy between the activity of mNTH1 and hNTH1. Alternatively, it is possible that the activities of hNTH1 to HOU and DHT were somehow kinetically masked due to the competition of multiple base lesions present in the γ-irradiated DNA substrate. The support for the latter possibility comes from the finding that hNTH1 indeed recognizes dihydrouracil in oligonucleotide substrates (*26*), a structural analogue of DHT.

Recently, a comparative study on the activity of Endo III for *cis*-TG and DHT has been reported by D'Ham et al. (*47*), showing that DHT is a poor substrate relative to *cis*-TG. The ratio of the V_{max}/K_m values for *cis*-TG vs DHT is 11:1, which qualitatively agrees with the present result (315:1) (Table 2). However, there are major parameter differences in reaching these conclusions. According to the reported study, k_{cat} values for *cis*-TG and DHT are 0.65 and 0.065 min^{-1}, respectively, with a 10-fold preference of *cis*-TG (both data calculated from reported V_{max}), whereas K_m is comparable for both damages (660 nM for TG and 680 nM for DHT). Therefore, k_{cat} is the exclusive determinant for the discrimination between *cis*-TG and DHT. In contrast, the present data indicate that both k_{cat} and K_m serve as discriminating factors and K_m (27-fold) exhibits a dominating effect rather than k_{cat} (11-fold). Although there are considerable variations, the K_m values of *E. coli* BER enzymes for good substrates are generally less than 50 nM (e.g., *48*−*50*). In view of these data, the reported K_m value for *cis*-TG (*47*) seems high as an affinity of Endo III for a good substrate. It has been suggested that *cis*-TG induces greater structural perturbations than DHT in duplex DNA. DHT, but not *cis*-TG, in templates allows translesion DNA synthesis efficiently (*38*, *51*, *52*), and the deoxyribonucleoside 5′-triphosphate of DHT, but not *cis*-TG, can replace dTTP as a substrate of DNA polymerases (*53*, *54*). The NMR studies also support this idea, showing that *cis*-TG induces a significant, localized structural change (*32*, *55*). Since structural alterations of DNA induced by aberrant bases play a key role in damage recognition of BER enzymes, it is reasonable to expect more tight binding of Endo III to *cis*-TG than DHT that induces much less perturbations. Unlike Endo III, *cis*-TG and DHT were incised with comparable efficiency by mNTH1. Based on the data in Table 2, it is tempting to speculate that upon binding to DNA, mNTH1 can induce more structural perturbations (bends or kinks) than Endo III in duplex DNA containing DHT, hence holding DNA tightly. This step is followed by a slow catalytic process, which seems virtually independent of the lesion structure (*cis*-TG or DHT).

Endo III has been suggested to extrude an aberrant base from a DNA helix into an active site pocket in the initial stage of base excision reaction (base flipping) (*14*). Granting this mechanism, the present results on the paired base effect suggest that *cis*-TG and DHT flip out the helix more readily when paired with G than A (Figure 8B,C, Table 2). The enhancement of the activity by G was particularly pronounced for DHT that stacked into the helix when paired with A. On the analogy of a T:G mispair, TG:G and DHT:G pairs are likely to form wobble base pairs in a helix (Figure 9B), whereas TG:A and DHT:A pairs mimic Watson−Crick

pairs (Figure 9A), albeit less stable than a T:A pair. In a T:G wobble base pair, T is shifted toward the major groove, and two hydrogen bonds are formed between guanine N1−H and thymine O2, and guanine O6 and thymine N3−H (*56*). The dislocation of *cis*-TG and DHT in a wobble base pair resembles that occurring in the initial stage of base flipping (i.e., partial activation of a substrate). If this is the case, a net free energy change before and after binding should be higher for the activated wobble pairs than Watson−Crick pairs, thereby resulting in the increase in the affinity (K_m) of Endo III for the wobble pairs (Table 2). In contrast to *cis*-TG and DHT, Endo III showed little preference of the paired base when UR and HOU were substrates. The NMR study on a duplex oligonucleotide containing UR implies that like abasic sites (*57*), the urea deoxyriboside can adopt an extrahelical position (*39*). Thus, spontaneous extrusion or flip-out of the urea deoxyriboside from a helix can overwhelm the passive effect conferred by the paired base. In addition, UR seems to be too small to interact with the opposite base in a helix. HOU might be also able to adopt an extrahelical position spontaneously since HOU (pK_a = 7.8, a ribonucleoside form) is partially ionized around neutral pH (*58*). Approximately one-third of HOU is estimated in an ionized form under the present experimental conditions (pH 7.5). The ionized species of HOU will tend to extrude from the hydrophobic helix core into water that provides a polar environment. For mNTH1, the paired base effect was not evident for *cis*-TG as well as UR and HOU, though a DHT:A pair was still discriminated (Figure 8E−H). If the perturbations conferred by mNTH1 upon binding to the substrate are large enough to extrude a damaged base (discussed above), the role of paired base will become less dominant. This may occur to TG paired with four bases and DHT paired with pyrimidines and G, but not to the most stable DHT:A pair.

ACKNOWLEDGMENT

We thank S. S. Wallace and Z. Hatahet for the generous gift of an *E. coli* strain for preparation of Endo III, and S. Nishimoto for the diastereoisomers of DHdT.

REFERENCES

1. Von Sonntag, C. (1987) *The Chemical Basis of Radiation Biology*, Taylor & Francis, New York.
2. Breen, A. P., and Murphy, J. A. (1995) *Free Radical Biol. Med. 18*, 1033−1077.
3. Ames, B. N. (1983) *Science 221*, 1256−1264.
4. Halliwell, B., and Gutteridge, J. M. C. (1989) *Free Radicals in Biology and Medicine*, 2nd ed., Oxford University Press, Oxford.
5. Wiseman, H., and Halliwell, B. (1996) *Biochem. J. 313*, 17−29.
6. Wallace, S. S. (1994) *Int. J. Radiat. Biol. 66*, 579−584.
7. Friedberg, E. C., Walker, G. C., and Siede, W. (1995) *DNA Repair and Mutagenesis*, ASM Press, Washington, DC.
8. David, S. S., and Williams, S. D. (1998) *Chem. Rev. 98*, 1221−1261.
9. Cunningham, R. P., and Weiss, B. (1985) *Proc. Natl. Acad. Sci. U.S.A. 82*, 474−478.
10. Asahara, H., Wistort, P. M., Bank, J. F., Bakerian, R. H., and Cunningham, R. P. (1989) *Biochemistry 28*, 4444−4449.
11. Bailly, V., and Verly, W. G. (1987) *Biochem. J. 242*, 565−572.
12. Kim, J., and Linn, S. (1988) *Nucleic Acids Res. 16*, 1135−1141.
13. Kuo, C. F., McRee, D. E., Fisher, C. L., O'Handley, S. F., Cunningham, R. P., and Tainer, J. A. (1992) *Science 258*, 434−440.
14. Thayer, M. M., Ahern, H., Xing, D., Cunningham, R. P., and Tainer, J. A. (1995) *EMBO J. 14*, 4108−4120.
15. Nash, H. M., Bruner, S. D., Sharer, O. D., Kawate, T., Addona, T. A., Spooner, E., Lane, W. S., and Verdine, G. L. (1996) *Curr. Biol. 6*, 968−980.
16. Jiang, D., Hatahet, Z., Blaisdell, J. O., Melamede, R. J., and Wallace, S. S. (1997) *J. Bacteriol. 179*, 3773−3782.
17. Sato, Y., Uraki, F., Nakajima, S., Asaeda, A., Ono, K., Kubo, K., and Yamamoto, K. (1997) *J. Bacteriol. 179*, 3783−3785.
18. Eide, L., Bjoras, M., Pirovano, M., Alseth, I., Berdal, K. G., and Seeberg, E. (1996) *Proc. Natl. Acad. Sci. U.S.A. 93*, 10735−10740.
19. Augeri, L., Lee, Y.-M., Barton, A. B., and Doetsch, P. W. (1997) *Biochemistry 36*, 721−729.
20. Roldan-Arjona, T., Anselmino, C., and Lindahl, T. (1996) *Nucleic Acids Res. 24*, 3307−3312.
21. Sarker, A. H., Ikeda, S., Nakano, H., Terato, H., Ide, H., Imai, K., Akiyama, K., Tsutsui, K., Bo, Z., Kubo, K., Yamamoto, K., Yasui, A., Yoshida, M. C., and Seki, S. (1998) *J. Mol. Biol. 282*, 761−774.
22. Aspinwall, R., Rothwell, D. G., Roldan-Arjona, T., Anselmino, C., Ward, C. J., Cheadle, J. P., Sampson, J. R., Lindahl, T., Harris, P. C., and Hickson, I. B. (1997) *Proc. Natl. Acad. Sci. U.S.A. 94*, 109−114.
23. Hilbert, T. P., Chaung, W., Boorstein, R. J., Cunningham, R. P., and Teebor, G. W. (1997) *J. Biol. Chem. 272*, 6733−6740.
24. You, H. J., Swanson, R. L., and Doetsch, P. W. (1998) *Biochemistry 37*, 6033−6044.
25. Bruner, S. D., Nash, H. M., Lane, W. S., and Verdine, G. L. (1998) *Curr. Biol. 8*, 893−903.
26. Ikeda, S., Biswas, T., Roy, R., Izumi, T., Boldogh, I., Kurosky, A., Sarker, A. H., Seki, S., and Mitra, S. (1998) *J. Biol. Chem. 273*, 21585−21579.
27. Dizdaroglu, M., Laval, J., and Boiteux, S. (1993) *Biochemistry 32*, 12105−12111.
28. Karahalil, B., Roldan-Arjona, T., and Dizdaroglu, M. (1998) *Biochemistry 37*, 590−595.
29. Senturker, S., Auffret van der Kemp, P., You, H. J., Doetsch, P. W., Dizdaroglu, M., and Boiteux, S. (1998) *Nucleic Acids Res. 26*, 5270−5276.
30. Dizdaroglu, M., Karahalil, B., Senturker, S., Buckley, T. J., and Roldan-Arjona, T. (1999) *Biochemistry 38*, 243−246.
31. Hatahet, Z., Kow, Y. W., Purmal, A. A., Cunningham, R. P., and Wallace, S. S. (1994) *J. Biol. Chem. 269*, 18814−18820.
32. Kao, J. Y., Goljer, I., Phan, T. A., and Bolton, P. H. (1993) *J. Biol. Chem. 268*, 17787−17793.
33. McNulty, J. M., Jerkovic., B., Bolton, P. H., and Basu, A. K. (1998) *Chem. Res. Toxicol. 11*, 666−673.
34. Sugiyama, H., Matsuda, S., Kino, K., Zang, Q.-M., Yonei, S., and Saito, I. (1996) *Tetrahedron Lett. 37*, 9067−9070.
35. Murakami, A., Tamura, Y., Ide, H., and Makino, K. (1993) *J. Chromatogr. 648*, 157−163.
36. Murakami, A., Tamura, Y., Wada, H., and Makino, K. (1994) *Anal. Biochem. 223*, 285−290.
37. Weinfeld, M., Liuzzi, M., and Paterson, M. C. (1989) *Nucleic Acids Res. 17*, 3735−3745.
38. Ide, H., Kow, Y. W., and Wallace, S. S. (1985) *Nucleic Acids Res. 13*, 8035−8052.
39. Gervais, V., Guy, A., Teoule, R., and Fazakerley, G. V. (1992) *Nucleic Acids Res. 20*, 6455−6460.
40. Gervais, V., Cognet, J. A. H., Guy, A., Cadet, J., Teoule, R., and Fazakerley, G. V. (1998) *Biochemistry 37*, 1083−1093.
41. Ide, H., Okagami, M., Murayama, H., Kimura, Y., and Makino, K. (1993) *Biochem. Mol. Biol. Int. 31*, 485−491.
42. Doetsch, P. W., and Cunningham, R. P. (1990) *Mutat. Res. 236*, 173−201.
43. Mazumder, A., Gerlt, J. A., Absalon, M. J., Stubbe, J., Cunningham, R. P., Withka, J., and Bolton, P. H. (1991) *Biochemistry 30*, 1119−1126.
44. Bally, V., and Verly, W. G., O'Connor, T. R., and Laval, J. (1989) *Biochem. J. 262*, 581−589.

45. Teebor, G., Cummings, A., Frenkel, K., Shaw, A., Voituriez, L., and Cadet, J. (1987) *Free Radical Res. Commn. 2*, 303−309.
46. You, H. J., Swanson, R. L., Harrington, C., Corbett, A. H., Jinks-Robertson, S., Senturker, S., Wallace, S. S., Boiteux, S., Dizdaroglu, M., Doetsch, P. W. (1999) *Biochemistry 38*, 11298−11306.
47. D'Ham, C., Romieu, A., Jaquinod, M., Gasparutto, D., and Cadet, J. (1999) *Biochemistry 38*, 3335−3344.
48. Purmal, A. A., Lampman, G. W., Bond, J. P., Hatahet, Z., and Wallace, S. S. (1998) *J. Biol. Chem. 273*, 10026−10035.
49. Tchou, J., Bodepudi, V., Shibutani, S., Antoshechkin, I., Miller, J., Grollman, A. P., and Johnson, F. (1994) *J. Biol. Chem. 269*, 15318−15324.
50. Asagoshi, K., Yamada, T., Terato, H., Ohyama, Y., Monden, Y., Arai, T., Nishimura, S., Aburatani, H., Lindahl, T., and Ide, H. (2000) *J. Biol. Chem. 275*, 4956−4964.
51. Ide, H., Petrullo, L. A., Hatahet, Z., and Wallace, S. S. (1991) *J. Biol. Chem. 266*, 1469−1477.
52. Evans, J., Maccabee, M., Hatahet, Z., Courcelle, J., Bockrath, R., Ide, H., and Wallace, S. S. (1993) *Mutat. Res. 299*, 147−156.
53. Ide, H., Melamede, R. J., and Wallace, S. S. (1987) *Biochemistry* 26, 964−969.
54. Ide, H., and Wallace, S. S. (1988) *Nucleic Acids Res. 16*, 11339−11354.
55. Kung, H. C., and Bolton, P. H. (1997) *J. Biol. Chem. 272*, 9227−9236.
56. Saenger, W. (1984) *Principles of Nucleic Acid Structure*, Springer-Verlag, New York.
57. Cuniasse, P., Fazakerley, G. V., Guschlbauer, W., Kaplan, B. E., and Sowers, L. C. (1990) *J. Mol. Biol. 213*, 303−314.
58. Fasman, G. D. (1975) *Handbook of Biochemistry and Molecular Biology. Nucleic Acids*, Vol. 1, CRC Press, Cleveland, OH.

BI000422L